

PAWEŁ KROCZAK \*, KONSTANTY SKALSKI \*\*, ANDRZEJ NOWAKOWSKI \*\*\*, ADRIAN MRÓZ \*\*\*\*

## THE ACCURACY OF THE REPRODUCTION OF THE LUMBAR SPINE ELEMENTS FOLLOWING CT AND MRI PROJECTIONS

The paper presents an analysis of factors influencing the accuracy of reproduction of geometry of the vertebrae and the intervertebral disc of the lumbar motion segment for the purpose of designing of an intervertebral disc endoprosthesis. In order to increase the functionality of the new type of endoprotheses by a better adjustment of their structure to the patient's anatomical features, specialist software was used allowing the processing of the projections of the diagnosed structures. Recommended minimum values of projection features were determined in order to ensure an effective processing of the scanned structures as well as other factors affecting the quality of the reproduction of 3D model geometries. Also, there were generated 3D models of the L4-L5 section. For the final development of geometric models for disc and vertebrae L4 and L5 there has been used smoothing procedure by cubic free curves with the NURBS technique.

This allows accurate reproduction of the geometry for the purposes of identification of a spatial shape of the surface of the vertebrae and the vertebral disc and use of the model for designing of a new endoprosthesis, as well as conducting strength tests with the use of finite elements method.

### 1. Introduction

Spine diseases, including, in particular, intervertebral disc diseases, constitute a serious health problem with a wide spectrum of social and economic

---

\* Instytut Obróbki Plastycznej, ul. Jana Pawła II 14, 61-131 Poznań, Poland; E-mail: kroczak@poczta.poznan.pl

\*\* Politechnika Warszawska, Zakład Konstrukcji Maszyn i Inżynierii Biomedycznej, ul. Narbutta 85, 02-524 Warszawa, Poland; E-mail: kskalski@wip.pw.edu.pl

\*\*\* Uniwersytet Medyczny im. Karola Marcinkowskiego, ul. Fredry 10, 61-701 Poznań, Poland;

\*\*\*\* Instytut Obróbki Plastycznej, ul. Jana Pawła II 14, 61-131 Poznań, Poland; E-mail: adrian.mroz@inop.poznan.pl

effects. Backaches accompanying a degenerative disease and resulting in the degeneration of mobility in many patients affect not only their quality of lives, but also availability at work [6]. Sick absence caused by the disease and the costs of treatment incur great expenses. It is estimated that almost half of the costs of health benefits are caused by backaches. The main reason for absence at work of people in the age group of up to 45 are backaches. As regards persons in the age group of 45+ who have experienced circulatory system diseases and degenerative disease, spine diseases are the most frequent causes of prescribed absences at work [8].

A development of imaging diagnostics and developmental trends in the adjustment of an implant to individual anatomical features and the patient's demands is today fundamental for the obtainment of satisfactory treatment results [11]. The results are supported by low- or non-invasive techniques that allow processing of the images from X-Ray CT projections or MRI projections [8]. This allows one to obtain geometrical data of biological structures enabling accurate reproduction of the same in 3D models [14].

They also enable identification of not only individual differences in relation to a typical geometry but also unique and pathological lesions in the internal structure of tissues [5].

The undertaken research was aimed at analyzing factors affecting the accuracy of the reproduction of the human lumbar spine as obtained from CT and MRI projections for the purposes of geometrical modeling of the spine segment structures as well as designing implants for the segments, for example, after intervertebral disc hernia.

One of the most advanced and significant imaging techniques using X-ray radiation properties is the above-mentioned Computer Tomography (CT) [13]. Following X-raying of a body and measuring the degree of absorption of X-rays by tissues of various densities, areas of diversified grayness are obtained. Tissues containing, for example, bodily fluids, absorb a larger part of radiation and are represented by gray areas (pixels) on the projection pictures. Flesh organs absorbing smaller radiation doses are represented by diversified shades of gray. Bony structures are characterized by high absorption and are represented by light areas on the pictures. The procedure for modeling of tissues from XT projections is shown in Fig. 1. Figure 1a and 1b depict CT projections and a method of display of the diagnosed structures in raster graphics. Figures 1c and 1d are related to the processing of images from projections including image segmentation [12], detection and conversion of data from projections into distribution of the absorption coefficient ( $\mu$ ). Figures 1d and 1e show the results obtained from geometrical modeling and modeling of material properties such as density or mechanical features ( $E$ ) (with the use of Hounsfield-HU scale).

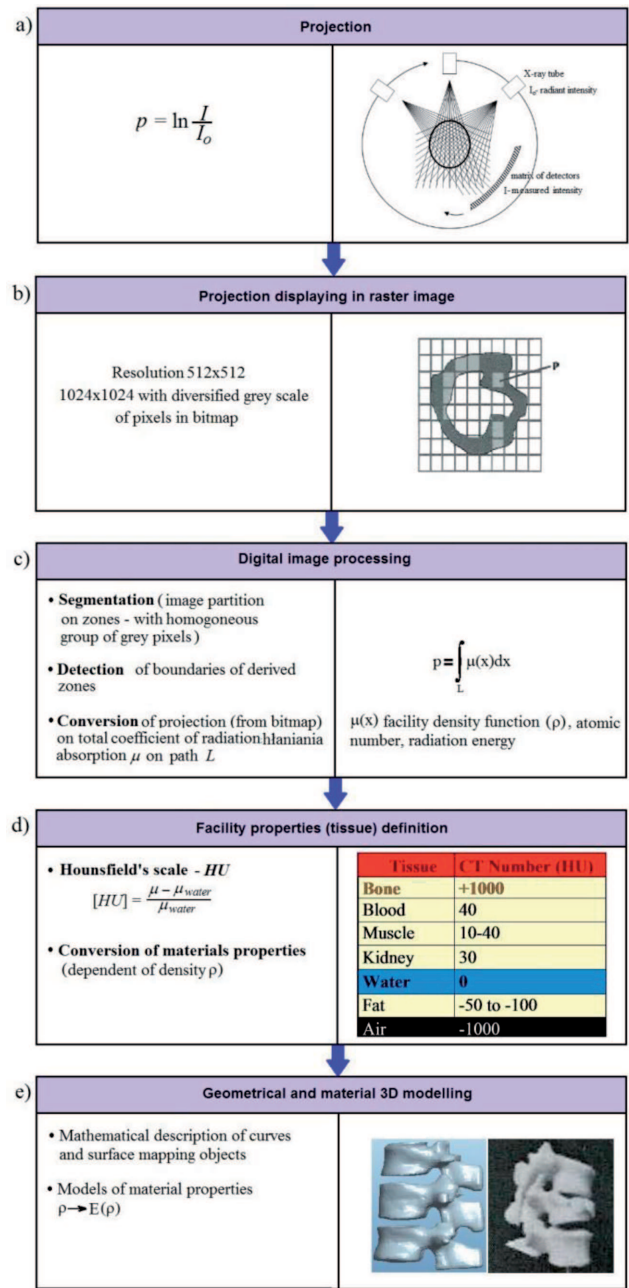


Fig. 1. The procedure for geometrical modeling of tissues on the basis of CT projection data

Magnetic Resonance Imaging is, beside CT, the most common method allowing imaging of internal structures of the human body and, in particular, his soft tissues. MRI test is practically non-invasive, as, contrary to X-ray examinations, it does not use X-ray radiation. Instead, it uses a magnetic

field and non-ionizing radiation with radio frequencies, which is not harmful to the organism [10]. The structures shown in the projections are mapped analogically in shades of gray depending on their density.

In practice, the CT and MRI instruments generate image information in a raster form. Files are recorded in the DICOM format [3]. The format is considered as universal for exchange of medical data.

On the basis of materials obtained from 75 CT and MRI tests of patients' lumbar spines, a database was developed. The collected group of CT and MRI projections constituted a valuable source for generating 3D models of L3-L5 motion segment and a basis for defining guidelines relating to the structures of intervertebral disc endoprosthesis.

The evaluation of accuracy of reproduction of the shape of human motion segment elements surface diagnosed with the use of CT and MRI methods is a difficult problem due to a variety of physical phenomena accompanying the above-mentioned diagnostic methods, and due to the method of processing and the technique of image presentation [14, 15]. On the basis of an analysis of literature and information obtained from manufacturers of CT and MRI diagnostic equipment, we may state that there are no unambiguous methods and strategies of determining the accuracy of the reproduction of the shape of bony structures [7, 8, 12] that are often impactful upon the functional correctness of the designed implants.

## 2. Materials and methods

The lumbar spine section is a section most exposed to degenerative lesions. At the height of the lumbar spine there is a center of gravity of the human body and, therefore, the forces influencing vertebrae and intervertebral discs at this height are the greatest. Most pathological lesions found in the vertebrae-intervertebral disc system relate to the L4-L5 section. Therefore, a database of clinical cases was created and it included CT and MRI test images (Fig. 2) for the L4-L5 section. Uniform sets related to a group of 52 patients (Table 1). The database structure was created in the form of folders with test results obtained from X-ray laboratories in three hospitals. The collected files contained basic data on each test. They included information about a patient (sex and age) as well as basic technical characteristics of the test such as, for example, the number of images, pixel size, image orientation, name of equipment used for the test, time and place of the test (Table 2).

In accordance with the assumptions, the developed database constituted a material for further analysis. It was used in the preferred order for construction of geometrical models thus enabling a design of a parametric and optimum geometry of an artificial disc.

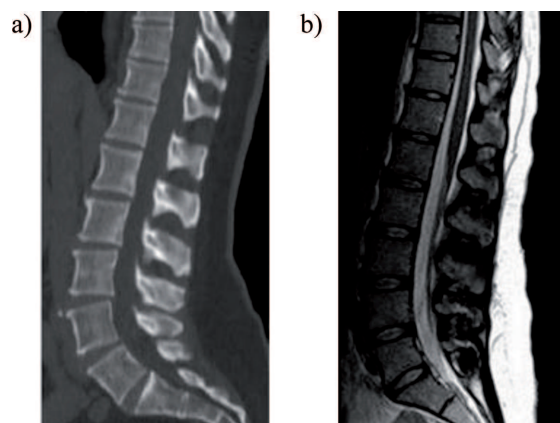


Fig. 2. Examples of spine images (medial cross-section) from the projection: a) CT with distinguished structures of cancellous and cortical bone tissue; b) MRI with visible intervertebral discs

Table 1.

Information concerning clinical cases collected in the database

Parameter	Value
Number of patients	52
women	31
men	21
Number of patients of unspecified age	7
Patient's minimum age	27
Patient's maximum age	82
Patient's average age	56,4
The median of patient's age	56
Number of patients below 45 years of age	9
Number of patients with CT projection	42
Number of patients with MRI projection	10

In the order of processing and after entering the data from the projection, preliminary segmentation of images followed in order to determine the bony tissue areas only.

In practice, the segmentation was performed by determining the HU boundary values with the use of a thresholding function (basic segmentation technique) that are stored in the form of 'masks' constituting one-color areas of diversified gray areas (Fig. 3).

It was insufficient to determine the boundary values for generating a geometrical model of the lumbar spine, as the generated mask has distortions

Table 2.  
 Information concerning properties of projections collected in the database of projections

Parameter	Value
Minimum pixel size	0.254 [mm]
Maximum pixel size	7.5 [mm]
Average pixel size	0.981499 [mm]
Minimum resolution	64×64 [pxl]
Maximum resolution	512×567 [pxl]
Minimum number of rasters	1
Maximum number of rasters	525
Minimum gap between rasters	0.6 [mm]
Maximum gap between rasters	14 [mm]
Minimum thickness of rasters	0.443 [mm]
Maximum thickness of rasters	10 [mm]

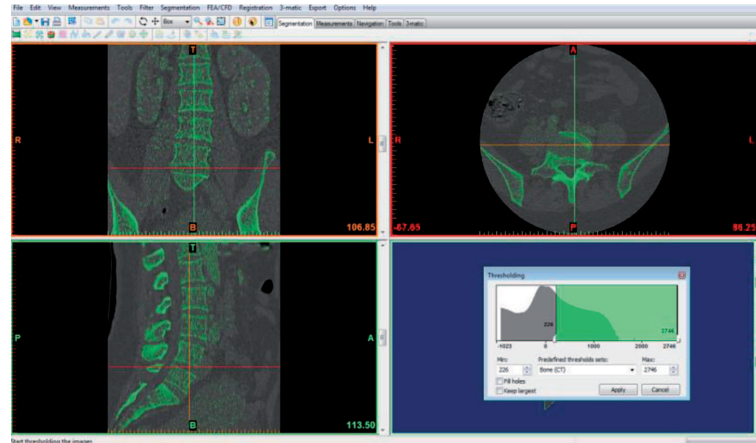


Fig. 3. Use of the thresholding function or creation of a 'mask'

of the actual shape of the bony structure. Therefore, the mask underwent a further modification as a result of which the distortions were removed and empty areas visible in Fig. 4 were filled in.

The modification was performed in numerous ways by using, *inter alia*, different commands of the specialized software. A manual edition was also possible. It involved adding or removing mask pixels with the use of a cursor. Figure 5 shows a model of L5 vertebra obtained from the mask edition. As a result, a solid model was obtained giving worse results in terms of the accuracy of the model reproduction.

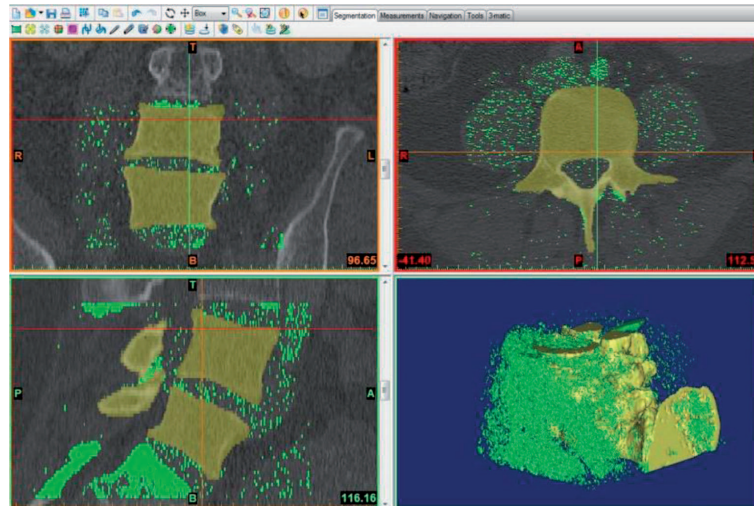


Fig. 4. Modification of the mask – elimination of distortions and filling of empty tissue areas

In the case of surface models of tissues and their approximation with the use of a finite elements grid, the accuracy of the reproduction of the tissue surfaces and their approximation with the use of fine elements grid greatly depends on the number of triangles in the grid.

The greater the number of triangles, the greater the accuracy of the reproduction of the tissue surfaces. However, there are problems with processing of irregular and considerably compacted grids. Modeling of tissues in this stage ends with a removal of irregularities and processing of models into the form of smooth surfaces (Fig. 5b).

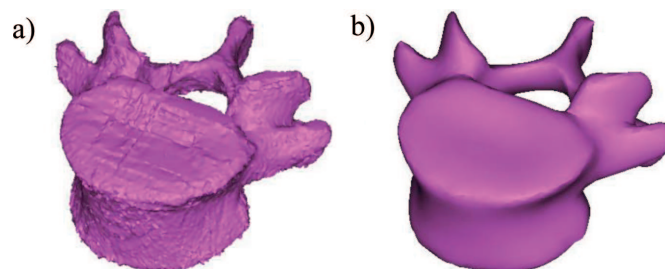


Fig. 5. 3D model of the L5 vertebral body: a) after completion of the mask edition, b) after smoothing

From the point of view of the tissue mechanical properties, a bone is a non-linear and slightly flexible material of complex anisotropic multilevel structure. An effective analysis of the bony structures requires considering the physical characteristics of individual types of bony tissues of vertebral bodies. In order to reproduce a non-uniform structure of the vertebral body,

in further activities areas were determined with the same material properties resulting from the density in accordance with the following relations [9]:

– material density  $\rho$  [ $\text{kg/m}^3$ ]

$$\rho(\text{HU}) = a_1 + a_2(\text{HU})^{a_3} + a_4(\text{HU})^{a_5} \quad (1)$$

– Young modulus  $E$  [MPa]

$$E(\rho) = b_1 + b_2(\rho)^{b_3} + b_4(\rho)^{b_5} \quad (2)$$

– Poisson coefficient  $\nu$  [–]

$$\nu(\rho) = c_1 + c_2(\rho)^{c_3} + c_4(\rho)^{c_5} \quad (3)$$

$a_i, b_i, c_i$  ( $i = 1, 2, \dots, 5$ ) – constants depending of the type of tissue tested.

### 3. Results

On the basis of images obtained from the CT and MRI projections, geometrical models of the bony structure of the L4–L5 intervertebral disc were generated. The geometry of the measurements is based upon the assumption that the generated element includes points, curves, surface patches and its dimensions [4] and shapes are obtained by appropriate approximations. From among the collected medical projections, only a part was suitable for effective modeling of the bony structures of the tested spine section.

Figure 6 presents an example of a spine section that, apart from the L4 and L5 vertebrae, also includes an intervertebral disc. In the case of projections derived from the MRI tests, it is possible to generate a direct image of the disc. The MRI technique is often recommended as a substitute for the CT technique, because, as already mentioned, it does not emit radiation harmful for human beings. However, a better resolution of the bony tissues structures in CT causes that the CT technique gives better opportunities in terms of obtaining data from the vertebrae geometry tests as shown in Fig. 2.

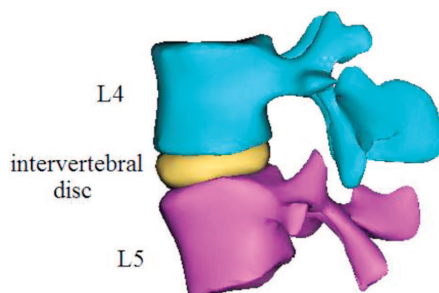


Fig. 6. The model of the L4-L5 section of the human spine

CT images indicated that intervertebral spaces are not filled in. Therefore, a decision was made to deliver a model of intervertebral disc with the use of one of the two indirect methods. The first method involved a manual edition of the intervertebral space and a use of 'Boolean operations' on the sets. The other method involved a creation of the geometrical disc model in the CAD system by 'stretching'. This approach indirectly uses the geometry of surfaces of the vertebral bodies adjacent to the disc, i.e. the bottom surface of the L4 body and the upper surface of the L5 body respectively.

3D geometries generated for the L4-L5 section of the human spine obtained from CT and MRI were presented in Figure 7 and 8 respectively.

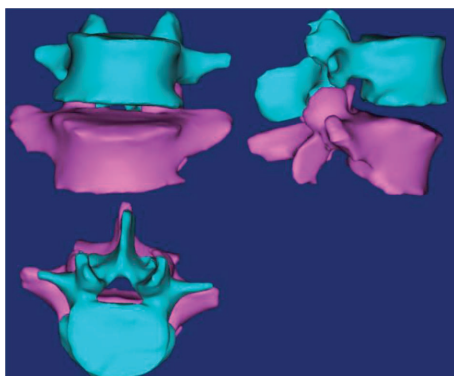


Fig. 7. A geometrical model obtained from a CT projection

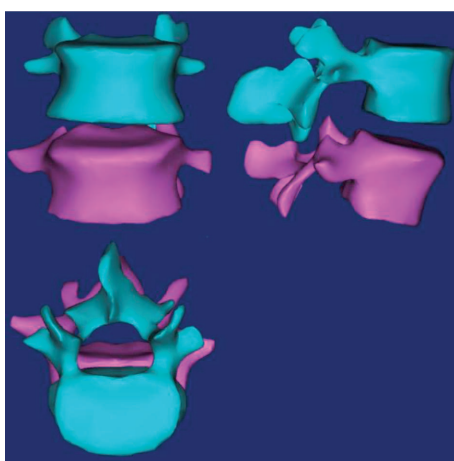


Fig. 8. A geometrical model obtained from an MRI projection

We may observe that the created vertebrae models have corrugated surfaces that are more visible after projections with the use of CT rather than MRI. However, the more correct the parameters of the projections with the use of CT, the more accurate the obtained model.

An undeniable advantage of modern techniques of non-invasive imaging as compared to the traditionally understood X-ray techniques, is a greater ability to create a 3D image of the tested tissue. This ability is ensured by the layered (raster) acquisition of data, i.e. images in parallel cross-sections. The number of rasters influences the quality of the geometry reproduction. The quality of the reproduction improves with an increase in the number of rasters, the positive effect of which is a decrease in the distance between the rasters (or a decrease in the raster thickness).

The above-mentioned values have a direct influence upon the quality of 3D modeling. It should be noted that the better the quality of the analyzed projections, the more pixels would the mask (created during thresholding) contain. The areas also correspond to diversified values of the Hounsfield's coefficient. They are characterized by smaller errors resulting from inaccurate covering of the area of a given tissue. Therefore, in this stage of modeling, it becomes necessary to undertake actions involving a mask modification. One of the methods of modification is the above-mentioned manual modification. In this stage of modeling, special attention should be devoted to the role of the human factor that has effects on the finally obtained geometry of the 3D model. The operator's experience, manual ability and the ability to perceive details are decisive factors in this case.

During attempts to map an intervertebral disc, we can observe mutual penetration (maladjustment) of the disc contours with the contours of the adjacent vertebral bodies. This phenomenon is caused by a diversified use of the smoothing functions in relation to the adjacent elements of the motion segment. The applied approximations result in a decrease in the number of elements reproducing the disc geometry. The level of the mutual maladjustment depends on the accuracy of the scanning in the projections and the selection of smoothing functions in modeling (Fig. 9).

The suitability of the individual projections for modeling is determined by basic parameters that have an influence upon the quality of the same. The parameters may include contrast, resolution, pixel size, number of rasters, distance between rasters and thickness of rasters as shown in Table 3.

It should be emphasized that contrast is a parameter determining the abilities to distinguish details. The greater the contrast, the better the presentation of the bone tissue. The ability to distinguish weakly contrasted structures in the projections (i.e. structures with small differences of HU coefficient values) is limited mainly by various types of distortions. The greatest unfavorable influence of the distortions may be observed in the case of objects with small contrast.

However, the resolution of the images determines their ability of distinguishing the locations of objects. A greater resolution also causes a lesser

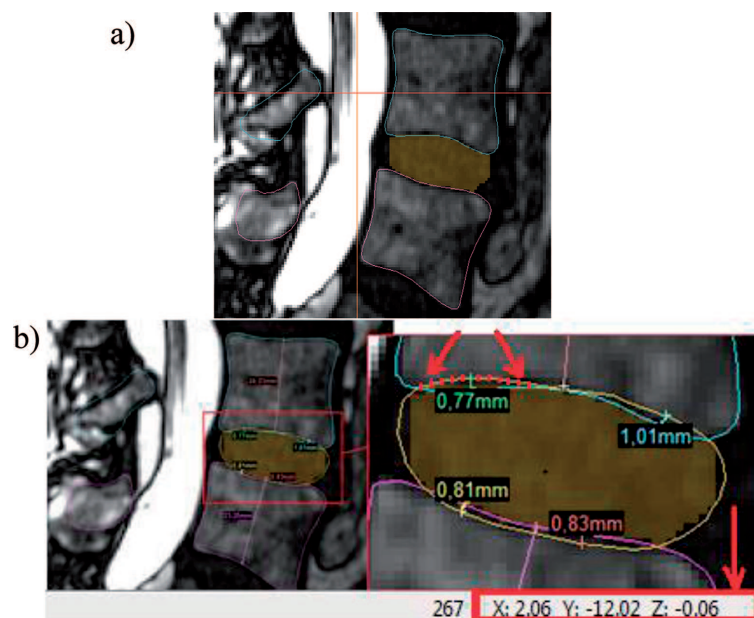


Fig. 9. Mutual penetration of contours of the intervertebral disc with adjacent surfaces of intervertebral bodies: a) before smoothing; b) after smoothing of the disc geometry and the nature of diffusion of curves

Table 3.

Comparison of the recommended basic property values determining the quality of the reproduction

Value		The lowest recorded value	The highest recorded value	Recommended value
<b>Resolution</b>	[pxl]	64×64	512×569	> 512×512
<b>Pixel size</b>	[mm]	0.254	7.5	< 0.5
<b>Number of rasters</b>	-	1	1002	As many as possible
<b>Distance between rasters</b>	[mm]	0	14	< 2.5
<b>Thickness of rasters</b>	[mm]	0.443	10	< 2.5

blurring effect and better visibility of tiny elements of the structure. A parameter affecting the resolution is the size of the pixel. The greater the resolution, the smaller the obtained pixel size.

In order to finally develop models of geometric contours of the disc and vertebral bodies there are proposed procedure for their smoothing by free cubic curves with NURBS technique. In the first step of this procedure, coordinates have been defined (based on tomographic projections) of the points x, y, z contours of the upper and lower contours of the disc and vertebral

bodies L4, L5, which are summarized in Table 4. In the next step, profile curves were formed by the interpolation technique parametric coordinates  $x(u)$ ,  $y(u)$ ,  $z(u)$ , which are presented in Fig. 10a.

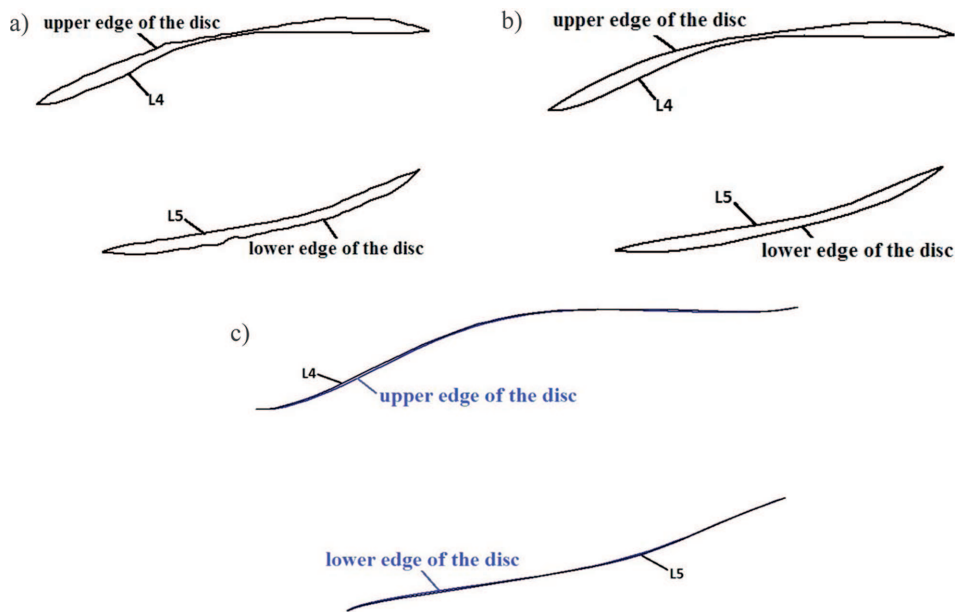


Fig. 10. a) Cubic curves interpolated by points  $x$ ,  $y$ ,  $z$  obtained from the computed tomography projection, b) smoothed curves, c) matching outlines of the disc to the outlines of the vertebral bodies

The number of NURBS control points of the contour was respectively upper/lower discs – 36/30, and for vertebral bodies L4/L5 – 36/31. The nature of diffusion of these curves (which can be seen) is consistent with the Fig. 9b.

In the next step, there was carried out smoothing profiles by reducing the number of control polygons points. This resulted in a smoother curves (Fig. 10b). A smaller number of control points in the individual polygons also simplifies potential modifications to the shape of the profiles. Number of control points of NURBS curves after modification was appropriate for the outline of the upper/lower disc – 6/5, and for sections L4/L5 – 10/9.

Matching contour profiles, i.e. respectively the upper and lower vertebral bodies L4 and L5 are shown in Fig. 10c. Matching was carried out by changing the positions of the control points  $D_i$ ,  $i = 0, 1, 2 \dots n$  of polygons measurable with vector functions parametric  $P(u)$  B-spline NURBS [1, 2].

Table 4.  
Coordinates points of the outline of the upper and lower pulley and the corresponding vertebral vertebrae obtained from tomographic projections

Item no.	section L4			upper edge of the disc			lower edge of the disc			section L4		
	x	y	z	x	y	z	x	y	z	x	y	z
1	<b>2,03</b>	<b>-5,65</b>	<b>0,05</b>	<b>2,03</b>	<b>-5,65</b>	<b>0,05</b>	<b>1,14</b>	<b>-6,25</b>	<b>-8,8</b>	<b>1,14</b>	<b>-6,25</b>	<b>-8,8</b>
2	2,02	-6,31	-0,06	2,05	-6,32	0,25	1,08	-6,94	-9,47	1,12	-6,88	-9,06
3	2,02	-7,01	-0,14	2,08	-7,05	0,45	1,03	-7,67	-10,01	1,1	-7,68	-9,31
4	2,02	-7,78	-0,15	2,1	-7,79	0,65	0,99	-8,37	-10,4	1,07	-8,38	-9,63
5	2,03	-8,48	-0,16	2,12	-8,46	0,75	0,97	-9,06	-10,68	1,05	-9,07	-9,88
6	2,03	-9,15	-0,13	2,13	9,19	0,78	0,95	-9,79	-10,94	1,03	-9,73	-10,17
7	2,04	-9,88	-0,14	2,13	-9,89	0,8	0,92	-10,39	-11,26	1	-10,47	-10,49
8	2,05	-10,58	-0,11	2,14	-10,59	0,8	0,9	-11,15	-11,54	0,98	-11,16	-10,78
9	2,06	-11,25	-0,08	2,15	-11,26	0,86	0,88	-11,78	-11,83	0,95	-11,82	-11,1
10	2,06	-11,98	-0,09	2,15	-11,99	0,81	0,86	-12,55	-12,01	0,93	-12,59	-11,35
11	2,07	-12,65	-0,07	2,15	-12,66	0,74	0,85	-13,25	-12,2	0,91	-13,22	-11,53
12	2,07	-13,42	-0,07	2,14	-13,39	0,59	0,84	-13,91	-12,34	0,9	-13,99	-11,79
13	2,08	-14,05	-0,08	2,14	-14,09	0,51	0,83	-14,62	-12,53	0,89	-14,65	-11,9
14	2,09	-17,78	-0,02	2,13	-14,79	0,43	0,82	-15,38	-12,64	0,88	-15,35	-12,05
15	2,1	-16,22	-0,07	2,13	-15,49	0,28	0,81	-16,11	-12,82	0,88	-16,01	-12,16
16	2,1	-16,88	-0,12	2,12	-16,29	0,21	0,8	-16,74	-12,97	0,87	-16,81	-12,31
17	2,09	-17,61	-0,23	2,11	-16,92	0,06	0,79	-17,51	-13,15	0,86	-17,48	-12,42
18	2,08	-18,31	-0,34	2,11	-17,62	-0,02	0,77	-18,17	-13,13	0,85	-18,18	-12,53
19	2,08	-18,98	-0,45	2,1	-18,25	-0,13	0,77	-18,8	-13,45	0,85	-18,91	-12,68
20	2,07	-19,71	-0,57	2,1	-18,98	-0,24	0,75	-19,49	-13,63	0,84	-19,57	-12,76
21	2,06	20,41	-0,71	2,09	-19,68	-0,36	0,76	-20,23	-13,67	0,84	-20,24	-12,87
22	2,05	-21,07	-0,9	2,09	-20,41	-0,47	0,75	-21	-13,82	0,83	-21,01	-12,98
23	2,03	-21,84	-1,15	2,08	-21,07	-0,62	0,74	-21,7	-13,9	0,82	-21,64	-13,1
24	2,01	-22,5	-1,44	2,07	-21,81	-0,73	0,74	-22,33	-14,01	0,82	-22,37	-13,24
25	1,98	-23,2	-1,79	2,07	-22,54	-0,81	0,73	23,09	-14,12	0,81	-23,07	-13,32
26	1,95	-23,93	-2,11	2,04	-23,2	-1,13	0,73	-23,79	-14,2	0,8	-23,8	-13,47
27	1,91	-24,62	-2,58	2,02	-23,9	-1,42	0,73	-24,49	-14,25	0,8	-24,54	-13,55
28	1,88	-25,28	-2,9	2	-24,6	-1,63	0,74	-25,12	-14,18	0,8	-25,2	-16,6
29	1,86	-25,98	-3,18	1,98	-25,33	-1,92	0,75	-25,12	-14,16	0,78	-25,9	-13,84
30	1,83	-26,71	-3,51	1,96	-26,03	-2,14	<b>0,77</b>	<b>-26,6</b>	<b>-14,06</b>	<b>0,77</b>	<b>-26,6</b>	<b>-14,06</b>
31	1,81	-27,41	-3,76	1,94	-26,69	-2,46						
32	1,79	-28,07	-4,01	1,92	-27,39	-2,71						
33	1,76	-28,77	-4,33	1,88	28,12	-3,1						
34	1,75	-29,5	-4,55	1,85	-28,78	-3,43						
35	1,74	-30,27	-4,66	1,83	-29,44	-3,71						
36	<b>1,74</b>	<b>-30,8</b>	<b>-4,7</b>	<b>1,74</b>	<b>-30,8</b>	<b>-4,7</b>						

$$P(u) = \frac{\sum_{i=0}^n w_i D_i N_{i,p}(u)}{\sum_{i=0}^n w_i N_{i,p}(u)} \quad (4)$$

where:  $w_i$  – weighting factors (0,1),  $N_{i,3}(u)$  – segment basis functions of cubic ( $p = 3$ ). The basic functions  $N_{i,3}(u)$  are generated by de Boor's algorithm for over nodes  $u_0, u_1, \dots, u_i \dots u_n$  according to the formulas:

$$N_{i,0}(u) = \begin{cases} 1 & \text{for } u_i \leq u \leq u_{i+1} \\ 0 & \text{otherwise} \end{cases}$$

$$N_{i,p=3}(u) = \frac{u - u_i}{u_{i+p} - u_i} N_{i,p-1}(u) + \frac{u_{i+p+1} - u}{u_{i+p+1} - u_{i+1}} N_{i+1,p-1}(u) \quad (5)$$

Consequently, the matching contours of the maximum deviation obtained according to:

- outline and contour of the upper disc and vertebral body L4 – approximately 0.15 mm,
- and the outline contour of the lower disc and vertebral body L5 – approximately 0.11 mm.

#### 4. Conclusions and comments

In order to increase the functionality of a new type of intervertebral disc endoprosthesis, structural solutions should be adjusted to the anatomical features. Therefore, the process of design and creation relating to a disc implant requires a delivery of 3D models of the L4–L5 motion segment of the spine.

On the basis of the obtained clinical materials obtained in the CT and MRI examinations, a database was developed forming a basis for the analysis of potential factors affecting the accuracy of the reproduction during geometrical modeling. The accuracy of the reproduction is greatly determined by the origin of the source files and the basic parameters determining their quality. The parameters include the contrast, the resolution, the pixel size, the number of rasters, the distance between the rasters and the thickness of the rasters. These factors also have a direct influence on the process of modeling of 3D geometrical models. The quality of the generated geometrical models is also determined by the human factor and the quality of hardware used by the operator.

The Minimum recommended values of the basic parameters have been presented in the paper. They characterize the images of the medical projections that determine their suitability for effective modeling of the bony structures, including the structure of the human intervertebral disc.

The results of the analysis may constitute a useful source of information regarding factors influencing the accuracy of the reproduction, attention to which should be drawn already in the stage of acquisition and collection of medical data.

Comparison of the results of smoothing and fitting (Fig. 9b and Fig. 10c) indicates the usefulness of NURBS technique in the final modeling the geometric outlines of the disc and vertebral bodies.

### Acknowledgements

The tests have been carried out as a part of the development project No. 13-0014-10 financed by NCBiR (National Center for Research and Development).

Manuscript received by Editorial Board, June 13, 2013;  
final version, September 03, 2014.

### REFERENCES

- [1] Farin G.E.: Curves and Surfaces for Computer Aided Geometric Design, Academic Press, 1995.
- [2] Piegl L., Tiller W.: The NURBS Book, Springer, Berlin, 1995.
- [3] Siczek M.: Tomografia komputerowa i rezonans magnetyczny dla studentów kierunku informatyka, Wydawnictwo Uniwersytetu Marii Curie-Skłodowskiej w Lublinie, Lublin 2011.
- [4] Skalski K., Grygoruk R., Werner A.: Grafika Komputerowa- Modelowanie geometryczne-laboratorium, Wpływ metod opisu krzywych i powierzchni na dokładność modelowania geometrycznego, Oficyna Wydawnicza Politechniki Warszawskiej, Warszawa, 2006, pp. 70-91.
- [5] Bagley L.J.: Imaging of Spinal Trauma, Radiol Clin N Am 44 (2006), pp. 1-12.
- [6] Lu Y.M., Hutton W.C., Gharpuray V.M.: Can variations in intervertebral disc height affect the mechanical function of the disc?, Spine, vol. 21, No. 19, 1996, pp. 2208-2217.
- [7] Olszewska M., Gąska A.: Porównanie różnych urządzeń metrologicznych wykorzystywanych w zastosowaniach biomedycznych, Postępy Nauki i Techniki, Nr 6, 2011, pp. 155-163.
- [8] Radziszewski K.R.: Analiza porównawcza aktywności zawodowej pacjentów z dyskopatią lędźwiową leczonych wyłącznie zachowawczo bądź operowanych, Wiadomości Lekarskie, 2007, LX, Nr 1-2, pp. 15-21.
- [9] Rho J., Hobatho M., Ashman B.: Relation of mechanical properties to density and CT number on human bone, Med. Eng. Phys. Vol. 17, No. 5, 1995, pp. 347-355.
- [10] Ryniewicz A.: Accuracy assessment of shape mapping using computer tomography, Metrology and Measurement Systems, Vol XVII (2010), Nr 3, pp. 481-492.
- [11] Skoworodko J., Skalski K., Kędzior K., Zagrajek T., Borkowski P.: Implant krążka międzykręgowego kręgosłupa lędźwiowego, Przegląd Lekarski, 2004/61, pp.147-150.

- [12] Skalski A.: Segmentacja 3D danych medycznych pochodzących z tomografii komputerowej oraz endoskopowych zapisów wideo, Rozprawa doktorska, Akademia Górniczo-Hutnicza im. Stanisława Staszica, Kraków 2009.
- [13] Brzeski P., Ćwiek D., Kędzior K., Skalski K., Smolik W., Szabatin R., Świeszkowski W.: Application of X – ray Computer Tomography to an Anthropometric Study of Elbow Joint bones, Proceed. 8th IMEKO BMI'98, Dubrownik, Croatia, September 1998, pp. 10-10÷10-13.
- [14] Świeszkowski W., Skalski K., Kędzior K., Werner A.: Przetwarzanie obrazów tomograficznych oraz modelowanie geometryczne kości stawów w systemie CAD, Mater. X. Konf. Naukowa Biocybernetyki i Inżynieria Biomedyczna, grudzień 1997, Warszawa, pp. 622-625.
- [15] Werner A., Skalski K., Kędzior K., Świeszkowski W.: Modelowanie geometryczne elementów układu kostnego człowieka z wykorzystaniem tomografii komputerowej i systemów CAD, Mater. I Sympozjum Inż. Ortopedyczna i Protetyczna, Białystok, czerwiec 1997, pp. 217-226.

#### **Dokładność odwzorowania elementów segmentu kręgosłupa lędźwiowego po projekcjach tomografii komputerowej i rezonansu magnetycznego**

##### Streszczenie

W artykule przedstawiono analizę czynników, które wpływają na dokładność odwzorowania geometrii kręgów i krążka międzykręgowego segmentu ruchowego kręgosłupa lędźwiowego, na potrzeby projektowania endoprotezy krążka międzykręgowego. W celu zwiększenia funkcjonalności nowego typu endoprotez poprzez lepsze dopasowanie ich konstrukcji do cech anatomicznych pacjenta, wykorzystywano specjalistyczne oprogramowanie, które umożliwiło przetwarzanie projekcji zdiagnozowanych struktur. Zgromadzone dane medyczne, pochodzące z projekcji tomografii komputerowej oraz rezonansu magnetycznego zostały opracowane i zestawione w utworzonej bazie danych. Poszczególne zbiory różniły się między sobą właściwościami (rozdzielczością, wielkością pojedynczego piksela, liczbą rastrów, odstępem pomiędzy rastrami oraz grubością rastrów). Na ich podstawie wygenerowano trójwymiarowe modele. Określono zalecane wartości minimalne cech projekcji, które zapewniają efektywne przetwarzanie skanowanych struktur oraz inne czynniki wpływające na jakość odwzorowania geometrii modeli 3D. Do końcowego opracowania modeli geometrycznych krążka oraz kręgów L4 i L5 wykorzystano procedurę wygładzania poprzez kubiczne krzywe swobodne techniką NURBS.

Dzięki temu możliwe jest dokładne odwzorowanie geometrii w celu identyfikacji przestrzennego kształtu powierzchni kręgów i krążka międzykręgowego oraz wykorzystania modelu do zaprojektowania nowej endoprotezy, a także do przeprowadzenia badań wytrzymałościowych metodą elementów skończonych.